Journal of Building Engineering 66 (2023) 105934

Contents lists available at ScienceDirect

Journal of Building Engineering

journal homepage: www.elsevier.com/locate/jobe

Estimation of indoor gamma radiation dose rate from concrete blocks constructed from tin mine tailings

I.O. Olarinoye [a,*], M.T. Kolo [a], H.O. Shittu [b], A.S. Anumah [a]

[a] Department of Physics, Federal University of Technology Minna, Nigeria
[b] National Agency for Science and Engineering Infrastructure (NASENI), Abuja, Nigeria

ARTICLE INFO

Keywords:
Concrete block
Specific activity
Nigerian room model
Dose rate
Buildup factor

ABSTRACT

The use of building materials made from geological sources contributes greatly to the indoor radiation exposure of human. As a result, it is critical for public health that building materials be screened for elevated radionuclide concentrations. This research measures the primordial radionuclide content of concrete blocks derived from mine tailings and also estimates the indoor annual effective dose rate (AEDR) and associated parameters. Furthermore, it presents a simple empirical relationship for evaluating dose rate per unit specific activity due to radionuclides from a wall of arbitrary dimensions. Twelve concrete blocks constructed using tin mine tailings as fine aggregates were collected locally and analyzed for ^{235}U, ^{232}Th and ^{40}K content using gamma spectrometry analysis. The concentration of ^{238}U ranged from 86.29 to 197.73 Bq/kg with a mean of 120.93 Bq/kg. Also, the specific activity of ^{232}Th and ^{40}K is within the limits: 99.01–353.67 Bq/kg and 500.71–1021.77 Bq/kg with mean values of 248.31 Bq/kg and 635.10 Bq/kg, respectively. Obtained dose rate per unit specific activity agreed well with data from literature. Using the derived values of dose rate per unit specific activity, the annual effective dose rate (AEDR) obtained from a typical Nigerian room varies significantly from that obtained from equations in referenced documents where a different room configuration was used. The mean AEDR from the realistic Nigerian room ($3.6 \times 3.6 \times 3$ m^3) was higher than the world average value but less than the recommended safety limit of 1 mSvy^{-1}. Some of the blocks with AEDR more than the safety limits were recommended for use in superficial quantities for building construction. The model derived in this study can be applied to calculate dose rates within any room configuration.

1. Introduction

Radiation has always been a human companion ever since man appeared in his environment. The risk associated with human exposure to ionizing radiation can never be eliminated but rather reduced [1]. This is due to the fact that radiation will continue to be present in the human environment. Sources of environmental radiation exposure to man may be categorized into natural and artificial sources [2]. The natural sources of radiation are inevitable as they are present in the human environment as cosmic radiation, whose exposure rate depends on geomagnetic latitude and altitude; terrestrial radiation, which emanates from primordial radionuclides such as isotopes of thorium, uranium, cesium, potassium, etc.; and internal radiation from ^{12}C and ^{40}K within man himself [2]. The terrestrial radiation exposure level often depends on the geology of the local environment, hence, exposure level varies with geography [3,4].

* Corresponding author.
E-mail addresses: leke.olarinoye@futminna.edu.ng, olarinoyeleke@gmail.com (I.O. Olarinoye).

https://doi.org/10.1016/j.jobe.2023.105934
Received 15 September 2022; Received in revised form 8 January 2023; Accepted 19 January 2023
Available online 20 January 2023

While the natural sources of radiation may be difficult to control, the artificial sources have always been regulated so that human exposure levels are as low as practicable. Environmental radiation level could be enhanced when the natural environment is perturbed by human activities such as mining and milling of minerals, excavations and the use of materials within high radiological content as raw materials for the construction of structures used for homes and offices [5]. The use of natural rocks, stones, or other geological formations directly or as raw materials for building materials is a major source of indoor radiation burden in the human environment. The radionuclide content of building materials comes primarily from primordial radionuclides, which are embedded in the natural rocks and raw materials from which these structural units are derived [6].

Concrete is a major building material whose applications cut across different economic strata. It is often used in large quantities for the construction of walls, floors, and sometimes roofs of structures that serve as homes, offices, business centers, places of worship, roads, road pavements, and others. Annually, the mean production of concrete per capita is 1 m^3 [7]. The widespread acceptance of concrete is predicated by the accessibility of the raw materials, its durability, mechanical strength, ease of production, low cost of production, minimal maintenance, and other benefits [8]. The major components required for making concrete are aggregates, cement, and water [5]; these are largely obtained from geological units. Being a product of geological formations, its radionuclide content is thus dependent on the description of the geological parameters of the materials from which the components were derived. Therefore, the specific radioactivity of concrete and other building materials fabricated from substances of different geological origin differs [2,7,9–12].

Furthermore, in order to reduce the cost of concrete production, the emission of greenhouse gases associated with cement production, and environmental problems due to the collection of aggregates and mineral rocks for cement production, there have been successful attempts to partially replace some of the main components required for concrete making with other materials. For instance, Estokova and Singovszka in 2021 [13] evaluated the radiological risk indices of cement mortar with different proportions of cement replaced by blast furnace slag (BFS) up to 95% by weight. The replacement was found to increase the specific activities of ^{40}K, ^{232}Th, and ^{238}U at different rates depending on the replacement level. Increasing BSF content in concrete has also been confirmed to increase the radionuclide concentration burden in cement mortars in other studies [14,15]. This was attributed to the higher specific activity of natural radionuclides in the BFS. As a way of recycling them, other industrial waste has been used as raw materials in the production of concrete [12,16–18]. It is therefore clear that the diversity in the indoor radiation level for structures constructed from concrete would depend on the nature or origin of the concrete materials.

To estimate the radiation induced risk associated with the use of building materials, it is essential that the radionuclide content of such materials be measured. This would help in determining the potential radiological risk associated with the use of the materials. It is expected that screening levels as recommended by local and international regulatory agencies will be used to discourage the use of highly radioactive building materials. Unfortunately, there is no radiological screening level for building materials that is prescribed and enforced by authorities in Nigeria. Consequently, building materials from diverse sources are used for construction without data on their radionuclide concentration levels.

Recently, [19] reported high ^{238}U, ^{232}Th, and ^{40}K concentrations in the mine soils and tailings of an active tin mine in the Jos area of Nigeria. Despite this finding, waste from this mine still continued to be used as aggregate for the construction of concrete blocks which are used for the construction of homes among low- and middle-class members of the Jos area. This could result in elevated radiation dose rate for the inhabitants of such structures. The fact that humans spend more than 50% of their time indoors suggests that the radiation exposure burden for the inhabitants of such structures cannot be ignored. Aside from medical exposure, building materials are the leading source of radiation exposure for humans [6]. These consequences motivated this study. The aim of this research is to estimate the radiological risk involved in the use of concrete blocks constructed from mine waste as building materials in the Jos area. The indoor annual effective dose in a typical model Nigerian room was also estimated and presented in this study. A simple empirical method for estimating dose rate within a building was also derived and applied in the report with the objective of continently estimating gamma dose rates due to inherent natural radionuclides in building materials for any room configuration. The derived method could be used to accurately screen building materials and room designs with the view of reducing indoor radiation exposure.

2. Materials and method

In order to ascertain the radiological safety of concrete blocks constructed using tailings from a mine, the blocks were collected and analyzed for their radiological content. The radiation safety indices of the blocks were calculated and their implications scrutinized. To obtain the actual dose received by individuals in a standard single room constructed from concrete, a mathematical model was constructed to obtain the dose rate from each wall in the standard room. The model was tested against previous models for validation. The details of the research methods are given in the sections below.

2.1. Sample collection and preparation

Twelve (12) concrete blocks whose fine aggregate could be traced to mine tailing collected in active and abandoned tin mines were collected in the Jos area of Nigeria. The block samples were crushed using agate mortar and sieved through a 500 μm mesh for particle size homogeneity. About 500 g of the samples were poured into 500 ml Marinelli beakers and sealed airtight to prevent radon gas from escaping from the sample. The samples were kept in the laboratory for 29 days to allow for secular equilibrium between ^{238}U and its progenies.

2.2. Activity measurement and spectra analysis

To measure the specific activity of the natural radionuclides: (^{238}U, ^{232}Th and ^{40}K) in the block samples, a gamma spectrometric

procedure was adopted. The spectrometric analysis was carried out with the use of a Canberra high purity germanium (HpGe) detector. The detector was housed in a 5 cm thick Pb cylindrical shield with an internal diameter of 24 cm and a height of 60 cm. The lead shield was lined with layers of 3 mm each of Cd and Plexiglas to provide additional shielding from external background radiation. The detector was coupled to a multi-channel analyzer card and PC for analyzing the photopeaks, which were accumulated over a period of 10 h. The energy resolution (full width at half maximum, FWHM) at 1.333 meV of the ^{60}Co gamma line was 0.0024 MeV, with a relative efficiency of 50%. The detector was calibrated using standard IAEA referenced source soils (RG U- 238), RG Th-332, RG K-40 with the same geometry and density as those of the pulverized block samples. The gamma spectra lines were carefully analyzed using Genie2000 spectroscopic software from Canberra by matching each photon energy peak to a gamma photon from specific radionuclides. The ^{238}U activity concentration was calculated indirectly from the gamma-ray peaks emitted by ^{214}Bi (609.31 and 1120.30 keV), while the 238.63 keV and 583.16 keV peaks from ^{212}Pb and ^{228}Ac gamma decay, respectively, were used to determine the concentration of ^{232}Th, and the single 1.46 MeV gamma line of ^{40}K was also used to determine the concentration of ^{40}K in the soil samples. The gamma-ray spectrum was accumulated and analyzed using Genie 2000 software.

The activity of the radionuclides was determined using Equation (1) [20].

$$A_i = \frac{C_n}{E_\gamma M_s I_\gamma} \tag{1}$$

where A_i is the activity concentration of the radionuclides (^{235}U, ^{232}Th, and ^{40}K) in the block samples, C_n is the net count per second of the sample under the corresponding photo-peak, E_γ is the efficiency of the detector at the specific gamma ray energy of interest, M_s is the mass of the assigned sample, and I_γ is the intensity of the gamma rays line of interest.

2.3. Evaluation of radiological dose and dose indices

As part of the radiological impact assessment of the ^{235}U, ^{232}Th, and ^{40}K concentrations in the concrete blocks, radiation dose and risk parameters are usually calculated. Different doses and hazard indices were estimated as follows.

2.3.1. Absorbed dose rate ($\dot{\mathbf{D}}$)

The absorbed dose rate ($\dot{D}$) in air due to the activity concentration of ^{238}U, ^{232}Th, and ^{40}K in the block sample was evaluated using Equation (2) [2,19,21].

$$\dot{D}\left(\mathrm{nGy}h^{-1}\right) = \sum_{i=1}^{3} A_i\, C_i \tag{2}$$

where A_i and C_i are the measured activity concentrations (Bq/kg) of ^{238}U, ^{232}Th and ^{40}K in the blocks and the dose rate conversion factor. C_i has values equal to 0.462, 0.604 and 0.0417 nGyh^{-1} per Bqkg^{-1} for ^{238}U, ^{232}Th and ^{40}K respectively.

2.3.2. Annual indoor effective dose rate ($AEDR_{in}$ (mSv/y))

The indoor annual effective dose rate received by an inhabitant of a structure made from the concrete block was estimated as given in Equation (3) [2].

$$AEDR_{in}\left(\frac{mSv}{y}\right) = \dot{D}\left(\frac{nGy}{h}\right) \times 8760\left(\frac{h}{y}\right) \times 0.8 \times 0.7 \times 10^{-6}\left(\frac{mSv}{nGy}\right) \tag{3}$$

2.3.3. Activity concentration index

The activity concentration index I is a parameter that could be used to screen building materials as radiologically safe or otherwise.

Table 1
Sample code, density and specific activity of ^{238}U, ^{232}Th, and ^{40}K in the concrete blocks.

Block sample	Density (kgm^{-3})	Specific activity (Bq/kg)		
		^{238}U	^{232}Th	^{40}K
CB1	2146	108.6 ± 19.78	353.67 ± 5.31	521.49 ± 89.39
CB2	2209	128.96 ± 11.32	285.8 ± 2.94	1021.77 ± 24.68
CB3	2150	103.05 ± 12.88	140.62 ± 6.56	500.71 ± 22.18
CB4	2120	109.8 ± 14.53	168.97 ± 17.77	542.48 ± 34.66
CB5	2145	86.29 ± 7.18	99.01 ± 9.85	597.17 ± 27.34
CB6	2143	99.91 ± 8.49	205.82 ± 9.87	516.6 ± 36.6
CB7	2145	107.32 ± 5.98	332.35 ± 10.87	617.55 ± 39.31
CB8	2123	128.79 ± 12.23	323.88 ± 2.88	1016.14 ± 56.24
CB9	2125	96.79 ± 17.23	221.62 ± 3.16	542.84 ± 68.33
CB10	2125	113.33 ± 16.68	318.1 ± 8.7	517.79 ± 34.42
CB11	2146	196.73 ± 9.23	221.46 ± 9.96	531.21 ± 15.23
CB12	2209	171.59 ± 7.29	308.38 ± 7.55	695.4 ± 23.37
Minimum	**2120**	**86.29**	**99.01**	**500.71**
Maximum	**2209**	**196.73**	**353.67**	**1021.77**
Mean	**2148.83**	**120.93**	**248.31**	**635.10**

The index for the building blocks was computed as follow [22]:

$$I = \frac{C_U}{300\ \left(\frac{Bq}{kg}\right)} + \frac{C_{Th}}{200\ \left(\frac{Bq}{kg}\right)} + \frac{C_K}{3000\ \left(\frac{Bq}{kg}\right)} \quad (4)$$

3. Results and discussion

3.1. Activity concentration

The activity concentrations of ^{238}U, ^{232}Th, and ^{40}K in the twelve considered concrete blocks as well as their respective densities are presented in Table 1. The concentration of ^{238}U ranged from 86.29 to 197.73 Bq/kg with a mean of 120.93 Bq/kg. Also, the specific activity of ^{232}Th and ^{40}K is within the limits: 99.01–353.67 Bq/kg and 500.71–1021.77 Bq/kg, with a mean value of 248.31 Bq/kg and 635.10 Bq/kg, respectively. These values show that the concentrations of the three radionuclides follow the order $C_K > C_{Th} > C_U$ for all the surveyed blocks. This pattern is consistent with that of mine tailing used in producing the blocks reported earlier [19]. Furthermore, the trend is consistent with the natural abundance of radioactive atoms in undisturbed soils [2,23]. This further suggests they could have originated from heavy mineral deposits in the mineral soil from which the tailing aggregates were derived (Bharath et al., 2022). The mean activity of the three radionuclides was well above the reported world average values of 30, 35, and 400 Bq/kg for ^{238}U, ^{232}Th and ^{40}K [24]. Furthermore, the radiological content of the present blocks is compared with similar concrete blocks from other parts of Nigeria and other countries in Table 2. Clearly, the mean activity concentrations of ^{238}U and ^{232}Th (120 and 248.31 Bq/kg, respectively) in the presently studied concrete blocks are higher than those from previous studies within and outside Nigeria. For instance, the concentrations obtained in this study for ^{238}U and ^{232}Th were 3.21 and 3.52 times greater than those obtained by Ademola in southwester Nigeria in 2008 and at least 2.78 and 5.2 greater than those obtained in Israel by Kovler et al. in 2002 (see Table 2). This point to ^{238}U and ^{232}Th rich minerals such which could only have come from the fine aggregate soil tailing used for the blocks fabrication. However, the specific activity of ^{40}K was found to be lower compared to that obtained from Finland and Israel. Based on the high radioactive content of the concrete blocks, their corresponding radiological safety parameters were estimated to ascertain their safety as building materials.

3.2. Radiological dose parameters

Diverse radiation dose quantities are often used to discriminate against the radiological risk associated with the use of materials for building. In this report, three parameters were computed for the purpose of evaluating the appropriateness of using concrete blocks for constructing homes. The absorbed dose rate, annual effective dose, and gamma dose index estimated via the use of Equations (2)–(4) are given in Table 3. The absorbed dose rate ranged from 124.57 to 297.5 nGy/h with a mean of 232.32 nGy/h. These translate to a mean indoor AEDE of 1.14 mSvy^{-1}. The dose rate of all the blocks exceeds the world averages for outdoor and indoor exposure of 45 and 84 nGh^{-1}, respectively [2]. These put the concrete blocks on the high side of the world average value of the radiation dose rate in building materials. Furthermore, more than half of the twelve blocks have an AEDE greater than the 1 mSv/y safety limit [32]. On the other hand, all the investigated concrete samples had an indoor AEDE value greater than the 0.41 mSv/y world average. These quantities suggest that the concrete blocks may not be ideal for building human residences, at least not in large quantities.

The activity concentration index I is used for screening materials that could exceed reference dose limits. Its value should be $\leq$ unity in order for dose limits not to be exceeded. Table 3 shows that only one sample had values of I less than unity. The index varies within the boundary 0.98–2.39. This makes the blocks appear unsuitable for building materials from a radiological health perspective. However, I may also be used to ascertain in what quantity a material may be used for building. It has been recommended that when the I is less than unity, the material can be used in bulk or in whatever quantity is desired for building. However, when the unity limit is exceeded, the material can only be used in superficial amounts [33]. These concrete blocks may be used in superficial quantities based on the gamma index. In addition, it has also been argued that precise dose valuation be carried out in such cases where the unity bound is exceeded. Such precision should take into account the density and thickness of the concrete in estimating indoor effective dose rate. Consequently, we examine a model for estimating the actual dose rate for an arbitrary room configuration.

Table 2
Comparison of specific activity of concrete blocks from different studies.

Location	Specific activity (Bq/kg)			Reference
	^{238}U	^{232}Th	^{40}K	
Cuba	–	12.00	595.00	[25]
Egypt	–	64.00	480.00	[26]
Finland	33.00	34.00	800.00	[9]
Ghana	9.80	20.50	107.00	[27]
Israel	42.90	47.70	870.10	[28]
Nigeria	29.00	26.00	289.00	[29]
Nigeria	24.50	37.30	354.40	[30]
Nigeria	37.30	70.50	339.00	[31]
Nigeria	120.00	248.31	635.10	Present study

Table 3
Dose parameters due to specific activity in the blocks.

Block sample	Dose parameters		
	D ($nGyh^{-1}$)	AEDE ($mSvy^{-1}$)	I_g
CB1	285.54	1.4	2.3
CB2	274.81	1.35	2.2
CB3	153.42	0.75	1.21
CB4	175.41	0.86	1.39
CB5	124.57	0.61	0.98
CB6	192.01	0.94	1.53
CB7	276.07	1.35	2.22
CB8	297.5	1.46	2.39
CB9	201.21	0.98	1.61
CB10	266.08	1.3	2.14
CB11	246.8	1.21	1.94
CB12	294.53	1.44	2.35
Minimum	**124.57**	**0.61**	**0.98**
Maximum	**297.5**	**1.46**	**2.39**
Mean	**232.32**	**1.14**	**1.86**

3.3. Indoor gamma dose within a standard room

Based on the fact that *I* exceed the unity limits, a more accurate dose evaluation technique that takes into consideration the quantity of blocks (density and thickness) used in the construction of a typical room in Nigeria is presented. Models that consider thickness and density have previously been put forward in previous studies; they failed due to thickness and density limitations [33]. In order to evaluate the absorbed dose rate due to the gamma ray source from natural sources in the concrete block, we derive an analytic expression for dose rate from a rectangular wall.

3.4. Dose calculation for an arbitrary rectangular wall configuration

Consider a rectangular wall with arbitrary dimensions L and B (Fig. 1) containing radioactive atoms emitting photons of energy E. To calculate the absorbed dose rate in air at P (a perpendicular distance H from the center of the wall surface), a cylindrical configuration was considered for simplicity, as shown in Fig. 2 [34]. Looking at an infinitesimal cylindrical source within the main cylindrical at Q. Let the volume and mass of the cylindrical element be:

$$dv = 2\pi r dr dt \tag{5}$$

$$dm = \rho dv = 2\pi\rho r dr dt \tag{6}$$

ρ is the density of the cylindrical wall. The specific activity A_m of wall element is

$$dA = A_m dm = 2\pi r \rho A_m dr dt \tag{7}$$

The dose rate at P due to the cylindrical element is:

$$d\dot{D} = \frac{\Gamma dA}{(x+y)^2} B e^{-(\mu_m y + \mu_a x)} \tag{8}$$

In **Equation (8)**, B is the photon buildup factor of the source material while μ_m and μ_a is the linear attenuation coefficient of the wall materials and air respectively. **Equation (8)**, has ignored photon buildup factor in air while the specific gamma constant of the radioactive isotope is Γ

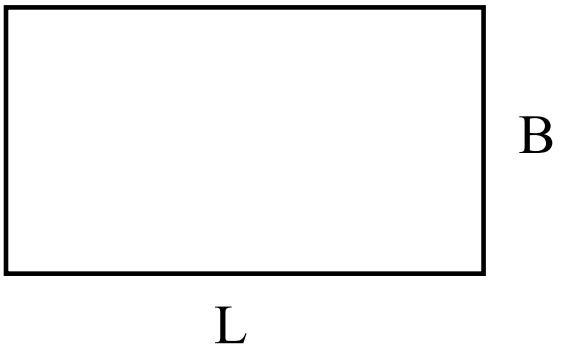

Fig. 1. Wall surface dimension.

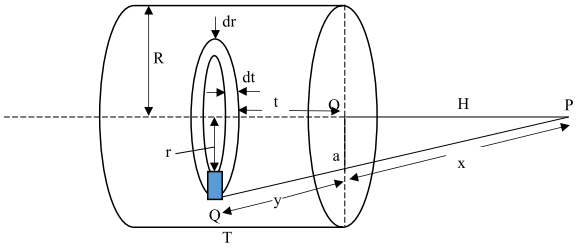

Fig. 2. Simplified cylindrical wall configuration.

For the entire wall, the total dose rate $\dot{D}$ is the integral of **Equation (8)** i.e.

$$\dot{D} = 2\pi\Gamma A_v \int_0^T \int_0^R \frac{rBe^{-(\mu_m y+\mu_a x)}}{(H+t)^2 + r^2} drdt \tag{9}$$

Ignoring attenuation in air and using the approximations: H » t and y ≈ t, A_v is the activity per unit volume.
For a thick source, **Equation (9)** becomes

$$\dot{D} = 2\pi\Gamma A_v \int_0^T \int_0^R \frac{rBe^{-\mu_c t}}{H^2 + r^2} dtdr \tag{10}$$

The solution to **Equation (10)** will depend on the form of B. If narrow beam transmission is assumed (B = 1), then,

$$\dot{D} = 2\pi\Gamma A_v \int_0^T \int_0^R \frac{re^{-\mu_c t}}{H^2 + r^2} dgdr$$

$$\dot{D} = \frac{2\pi\Gamma A_v}{\mu_c}\left(1 - e^{-\mu_c T}\right) \int_0^R \frac{rdr}{H^2 + r^2}$$

The integral, $\int_0^R \frac{rdr}{H^2 + r^2} = \frac{1}{2}\ln\left(\frac{H^2 + R^2}{H^2}\right)$,

Hence,

$$\dot{D} = \pi\Gamma A_v \left(\frac{1 - e^{-\mu_c T}}{\mu_c}\right) \ln\left(\frac{H^2 + R^2}{H^2}\right)$$

$$\dot{D} = \pi\Gamma A_m \rho \left(\frac{1 - e^{-\mu_c T}}{\mu_c}\right) \ln\left(\frac{H^2 + R^2}{H^2}\right) \tag{11}$$

Considering a linear form of B i.e. $B = 1 + \mu_c t$ [35], **Equation (10)** becomes

$$\dot{D} = 2\pi\Gamma A_v \int_0^T \int_0^R \Gamma \frac{(1 + \mu_c t)}{H^2 + r^2} e^{-\mu_c t} dtdr$$

$$\dot{D} = \pi\Gamma A_v \, ln\left(\frac{H^2 + R^2}{H^2}\right) \int_0^T (1 + \mu_c t)\, e^{-\mu t} dt$$

Take $I_1 = \int_0^T e^{-\mu g} dt = \frac{1 - e^{-\mu_c T}}{\mu}$

$$I_2 \int_0^T \mu_c t e^{-\mu_c t} dt = \frac{1}{\mu_c}\left[1 - (1 + \mu_c T) e^{-\mu_c T}\right]$$

$$\dot{D} = \pi\Gamma A_m \rho \, ln\left(\frac{H^2 + R^2}{H^2}\right)\left(\left(\frac{1 - e^{-\mu_c T}}{\mu_c}\right) + \left(\frac{1 - (1 + \mu_c T) e^{-\mu_c T}}{\mu_c}\right)\right)$$

$$\dot{D} = \frac{\pi\Gamma A_m \rho}{\mu_c} ln\left(\frac{H^2 + R^2}{H^2}\right).\left(2\left(1 - e^{-\mu_c T}\right) - \mu_c T e^{-\mu_c T}\right) \tag{12}$$

The new term: $\left(\frac{1 - (1+\mu_c T) e^{-\mu_c T}}{\mu_c}\right)$ accounts for the effect of B hence the multiplier accounting for multiple scattering within the cylindrical wall of thickness G. The specific gamma constant for the radionuclide is estimated as:

$$\Gamma = \frac{1}{4\pi}\sum Y_i E_i \left(\mu_{en}/\rho\right)_i \tag{13}$$

E_i is the energy of the emitted photon with emission uncertainty of Y_i while (μ_{en}/ρ) is the mass energy absorption coefficient of air at E_i.

In real situations, walls are actually rectangular in shape. Hence our model wall in Fig. 2 must have the same volume of radioactive material as the rectangular wall of thickness T in Fig. 1. In terms of the rectangular wall dimension, the radius R in **Equations 11** and **12** is [36]:

$$\mathrm{R} = \frac{A}{P}\sqrt{\frac{16}{\pi}} \tag{14}$$

where A and P represent the area and perimeter of the wall, respectively.

3.5. Validation of theory

To validate this model, the dose at the center of a typical room constructed with ordinary concrete with dimensions $5 \times 4 \times 2.8\ \mathrm{m}^3$ was estimated. The room has walls, floors, and a roof with a thickness of 20 cm and a density of $2.32\ \mathrm{g\ cm}^2$. Using the energy spectrum for ^{238}U, ^{232}Th, and ^{40}K as given in [[9,37], the dose rate per unit (mass) specific activity $\dot{\mathrm{D}}/A_m$ based on **Equations 11** and **12** for the standard room was estimated, and the result is given alongside those obtained from Monte Carlo simulations and other models in Table 4. Clearly, the values obtained using the analytic expression in this work agree well with previous approaches. The fine line between the values obtained herein and previous works could be attributed to the simplified buildup expression adopted in this work and the gamma photon energies included in the ^{238}U and ^{232}Th series decays in the computation. The influence of the multiple scattering of photons within the walls is obvious when $\dot{\mathrm{D}}/A_m$ obtained through **Equations 11** and **12** are compared. There was an increase of about 76%, 74%, and 55% in the value of dose rate per activity for ^{238}U, ^{232}Th, and ^{40}K respectively, when photon buildup is considered. The observed increase could be higher for thicker walls. The method highlighted in this study is simple and better if the effects of specific room details such as windows, doors, and different roof materials are to be considered, unlike in the volume integral expressions used by other authors in the past [9–11].

Using the derived **Equation (11)** and **12,** the dose rate at the middle of a standard Nigerian room of dimensions $3.6 \times 3.6 \times 3.0\ \mathrm{m}^3$ with and without a standard size single window and door is estimated. The thickness of the concrete blocks, with a mean density of $2148.83\ \mathrm{kgm}^{-3}$ (Table 1) was taken as 10 cm. The obtained $\dot{\mathrm{D}}/A_m$ for Nigerian room with (NRWB) and without photon buildup (NRNB) is compared with that of a standard room size ($5 \times 4 \times 2.5\ \mathrm{m}^2$) with (SRWB) and without (SRNB) buildup factor in Fig. 3. Obviously, the coefficients obtained using a standard room overestimate the dose coefficients. The dose coefficient $\dot{\mathrm{D}}/A_m$ for NRNB is 0.035, 0.407, and 0.339 $\mathrm{nGyh}^{-1}/\mathrm{Bqkg}^{-1}$ for ^{4} K, ^{232}Th, and ^{238}U respectively, with corresponding values of 0.035, 0.489, and 0.418 $\mathrm{nGyh}^{-1}/\mathrm{Bqkg}^{-1}$ for NRWB. Using the $\dot{\mathrm{D}}/A_m$ for NRWB in **Equation (2)**, the dose rate due to the radionuclides in the concrete blocks was estimated and shown in Fig. 4. The obtained dose rates vary within the range of 105.44–247.90 nGyh^{-1} with a mean of 194.31 nGyh^{-1}. The figure shows that the dose rates from all the sampled concrete blocks were above the world average value (shown with yellow solid line). However, the dose rate evaluated from the literature value of $\dot{\mathrm{D}}/A_m$ [2,19,21] is overestimated. The dose rate obtained for a typical Nigerian room thus presents a more realistic value. Similarly Using **Equation (3)**, the AEDR for a NRWB was estimated and shown in Fig. 5. Clearly, the more realistic Nigerian room configuration reduced the AEDR to within the safety limit of 1 mSv/y (red solid line) for all the blocks. However, the obtained AEDR is elevated compared to the World average value. The obtained mean AEDR reflects a more realistic value compared to using standard equations that did not consider Nigerian room configuration as shown in Table 3. Other radiation safety parameters such as gonadal dose and excess lifetime cancer risk could thus be calculated from the $\dot{\mathrm{D}}/A_m$ and AEDR estimated using a realistic room configuration. It must be noted that the dose rate obtained in this study represents the peak dose rate as the provision of window, door, and using a roofing material other than concrete with lower radionuclide content will further reduce the dose level at the center of the room. To account for windows and doors where available, the absorbed dose due to a wall configuration similar to the window and door will be subtracted for either the corresponding wall or that of the entire room. The

Table 4
Gamma specific dose rate compared for different studies and methods for a $5 \times 4\text{x}2.8\ \mathrm{m}^3$ room with wall, floor and roof thickness of 20 cm.

Gamma dose rate nGyh^{-1} $(\mathrm{Bqkg}^{-1})^{-1}$			Wall density (gcm^{-3})	Method	References
^{238}U	^{232}Th	^{4} K			
0.467	0.568	0.052	2.35	Equation 11	This study
0.823	0.986	0.08	2.35	Equation 12	This study
0.88	1.08	0.079	2.35	Monte Carlo (MCNP5)	[37]
1.08	1.22	0.09	2.3	Hybrid Monte Carlo	[38]
0.92	1.24	0.084	2.35	Analytic	[11]
0.7	0.92	0.072	2.35	Analytic	[10]
0.93	1.1	0.081	2.35	Analytic	[9]

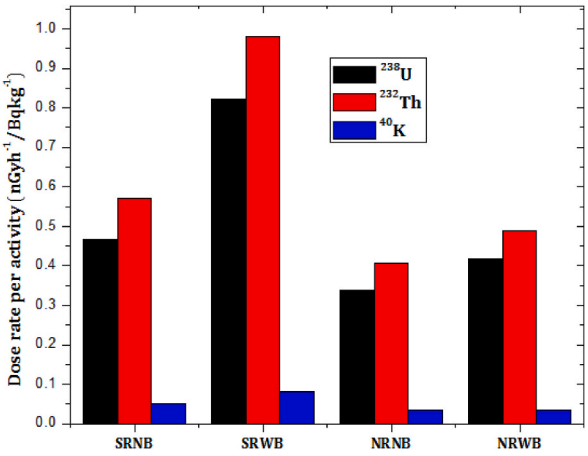

Fig. 3. Dose rate per unit activity compared for standard and typical Nigerian rooms.

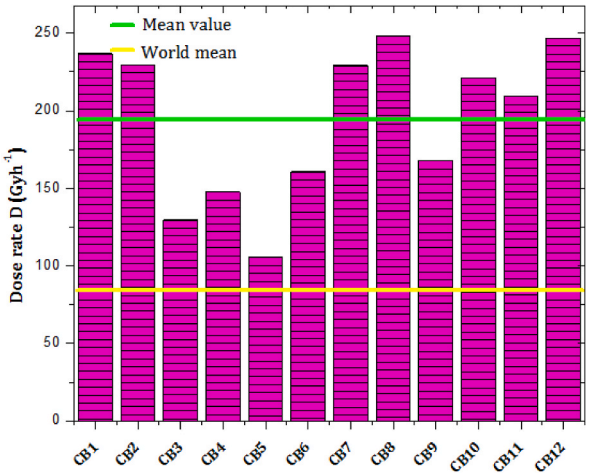

Fig. 4. Dose rate due to radionuclide content of the investigated concrete blocks.

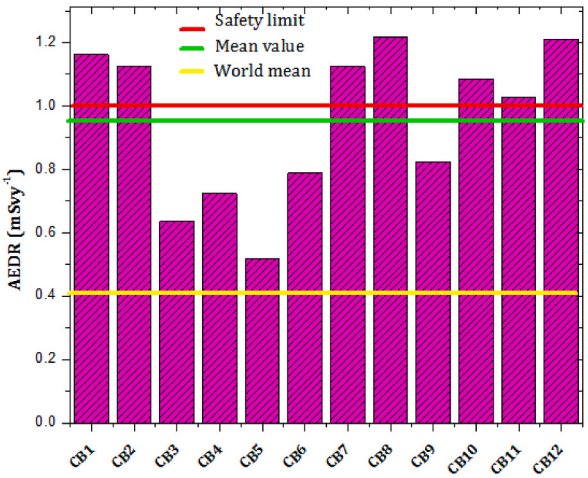

Fig. 5. Indoor AEDR of a Nigerian room constructed from the investigated concrete blocks.

inclusion of radiation attenuation in air which was ignored in this dose calculation model, could further reduce the dose received from the concrete blocks.

4. Conclusion

Twelve concrete blocks made using tailings from a tin mine were analyzed for their primordial radionuclide content. Using a well calibrated HpGe detector, the mean concentration of ^{238}U, ^{232}Th, and ^{40}K was 120.93 Bq/kg, 248.31 Bq/kg and 635.10 Bq/kg accordingly. The evaluated dose rate per unit (mass) specific activity $\left(\dot{D}/A_m\right)$ varies with radionuclide and also depends on photon buildup factor. Using the derived $\dot{D}/A_m$ the annual effective dose rate vary significantly from those obtained using conventional expressions. The dose coefficient $\dot{D}/A_m$ for NRNB was 0.035, 0.407, and 0.339 nGyh^{-1}/Bqkg^{-1} for ^{40}K, ^{232}Th, ^{238}U respectively with a corresponding values of 0.035, 0.489, and 0.418 nGyh^{-1}/Bqkg^{-1} for NRWB. Also, the obtained dose rates vary within the range of 105.44–247.90 nGyh^{-1} with a mean of 194.31 nGyh^{-1}. The model presented in this work could be used to estimate dose rate at the center or any point within any arbitrary room dimension with good accuracy and allows for the subtraction of dose due to the provision of windows and doors. The AEDR of the 10 blocks had a mean of 0.953 mSv/yr which is less than the safety limit. Some of the blocks have an AEDR higher than 1 mSv/annum, hence making them radiologically unsafe for construction purposes. They are recommended to be used in superficial quantities for construction.

Author statement

The authors are grateful to the Department of Physics, Federal University of Technology, Minna, for allowing access to its facility.

Declaration of competing interest

The authors declare that they have no known competing financial interests or personal relationships that could have appeared to influence the work reported in this paper.

Data availability

No data was used for the research described in the article.

References

[1] W. Schimmerling, F.A. Cucinotta, J.W. Wilson, Radiation risk and human space exploration, Adv. Space Res. 31 (1) (2003) 27–34.
[2] UNSCEAR (United Nations Scientific Committee on the Effects of Atomic Radiation), Sources and Effects of Ionizing Radiation, ANNEX B, Exposures from Natural Radiation Sources, vol. 1, UNSCEAR 2000 REPORT, New York, 2000, pp. 97–99.
[3] I.O. Olarinoye, I. Sharifat, A. Baba-Kutigi, M.T. Kolo, K. Aladeniyi, Measurement of background gamma radiation levels at two tertiary institutions in minna, Nigeria, J. Appl. Sci. Environ. Manag. 14 (1) (2010).
[4] M. Belivermis, Ö. Kılıç, Y. Çotuk, S. Topcuoğlu, The effects of physicochemical properties on gamma emitting natural radionuclide levels in the soil profile of Istanbul, Environ. Monit. Assess. 163 (1) (2010) 15–26.
[5] O.I. Olarinoye, M.M. Idris, M. Kure, Photon and fast neutron transmission parameters of metakaolin doped concrete, *Journal of Building Material Science*| 3 (2021), 02.
[6] E.O. Agbalagba, R.O.A. Osakwe, I.O. Olarinoye, Comparative assessment of natural radionuclide content of cement brands used within Nigeria and some countries in the world, J. Geochem. Explor. 142 (2014) 21–28.
[7] K. Kovler, The national survey of natural radioactivity in concrete produced in Israel, J. Environ. Radioact. 168 (2017) 46–53.
[8] L.R. Caldas, A.B. Saraiva, A.F. Lucena, M.H.Y. Da Gloria, A.S. Santos, R.D. Toledo Filho, Building materials in a circular economy: the case of wood waste as CO2-sink in bio concrete, Resour. Conserv. Recycl. 166 (2021), 105346.
[9] R. Mustonen, Methods for evaluation of radiation from building materials, Radiat. Protect. Dosim. 7 (1–4) (1984) 235–238.
[10] M.F. Máduar, G. Hiromoto, Evaluation of indoor gamma radiation dose in dwellings, Radiat. Protect. Dosim. 111 (2) (2004) 221–228.
[11] J.A. Ademola, I.P. Farai, Annual effective dose due to natural radionuclides in building blocks in eight cities of southwestern Nigeria, Radiat. Protect. Dosim. 114 (4) (2005) 524–526.
[12] A. Estokova, E. Singovszka, M. Vertal, Investigation of building materials' radioactivity in a historical building—a case study, Materials 15 (2022) 6876.
[13] A. Estokova, E. Singovszka, Assessment of risk from irradiation originating from mortars with mineral waste addition, Indoor Built Environ. 31 (1) (2022) 219–229.
[14] H. Binici, O. Aksogan, A.H. Sevinc, A. Kucukonder, Mechanical and radioactivity shielding performances of mortars made with colemanite, barite, ground basaltic pumice and ground blast furnace slag, Construct. Build. Mater. 50 (2014) 177–183.
[15] K. Manikanda Bharath, U. Natesan, S. Chandrasekaran, S. Srinivasalu, Determination of natural radionuclides and radioactive minerals in urban coastal zone of South India using Geospatial approach, J. Radioanal. Nucl. Chem. (2022) 1–14.
[16] N. Stevulova, V. Vaclavik, J. Junak, R. Grul, M. Bacikova, Utilization possibilities of selected waste kinds in building materials preparing, *International Multidisciplinary Scientific GeoConference*: SGEM 2 (2008) 193.
[17] H.M. Saleh, A.A. Salman, A.A. Faheim, A.M. El-Sayed, Sustainable composite of improved lightweight concrete from cement kiln dust with grated poly (styrene), J. Clean. Prod. 277 (2020), 123491.
[18] H.M. Saleh, A.A. Salman, A.A. Faheim, A.M. El-Sayed, Influence of aggressive environmental impacts on clean, lightweight bricks made from cement kiln dust and grated polystyrene, Case Stud. Constr. Mater. 15 (2021), e00759.
[19] M. Atipo, O. Olarinoye, B. Awojoyogbe, Comparative analysis of NORM concentration in mineral soils and tailings from a tin-mine in Nigeria, Environ. Earth Sci. 79 (16) (2020) 1–17.
[20] M.M. Orosun, M.R. Usikalu, K.J. Oyewumi, J.A. Achuka, Radioactivity levels and transfer factor for granite mining field in Asa, North-central Nigeria, Heliyon 6 (6) (2020), e04240.
[21] H.T. Abba, W.M.S.W. Hassan, M.A. Saleh, Evaluation of environmental natural radioactivity levels in soil and ground water of Barkin Ladi, Plateau state, Nigeria, Malaysian Journal of Fundamental and Applied Sciences 14 (3) (2018) 338–342.

[22] IAEA Safety Standards Series; no. SSG-32; May 2015; 112 p; IAEA; Vienna (International Atomic Energy Agency (IAEA)); STI/PUB–1651; ISBN 978-92-0-102514-2; Worldcat; ISSN 1020-525X.
[23] D.A. Schauer, O.W. Linton, National Council on Radiation Protection and Measurements report shows substantial medical exposure increase, Radiology 253 (2) (2009) 293–296.
[24] L. Gaspar, I. Lizaga, A. Navas, Spatial distribution of fallout and lithogenic radionuclides controlled by soil carbon and water erosion in an agroforestry South-Pyrenean catchment, Geoderma 391 (2021), 114941.
[25] O.B. Flores, A.M. Estrada, R.R. Suárez, J.T. Zerquera, A.H. Pérez, Natural radionuclide content in building materials and gamma dose rate in dwellings in Cuba, J. Environ. Radioact. 99 (12) (2008) 1834–1837.
[26] N.K. Ahmed, Measurement of natural radioactivity in building materials in Qena city, Upper Egypt, J. Environ. Radioact. 83 (1) (2005) 91–99.
[27] F. Otoo, E.O. Darko, M. Garavaglia, C. Giovani, S. Pividore, A.B. Andam, S. Adu, Public exposure to natural radioactivity and radon exhalation rate in construction materials used within Greater Accra Region of Ghana, Scientific African 1 (2018), e00009.
[28] K. Kovler, G. Haquin, V. Manasherov, E. Ne'eman, N. Lavi, Natural radionuclides in building materials available in Israel, Build. Environ. 37 (5) (2002) 531–537.
[29] K. Aladeniyi, A.M. Arogunjo, A.J.S.C. Pereira, M.U. Khandaker, D.A. Bradley, A. Sulieman, Evaluation of radiometric standards of major building materials used in dwellings of South-Western Nigeria, Radiat. Phys. Chem. 178 (2021), 109021.
[30] J.A. Ademola, P.O. Oguneletu, Radionuclide content of concrete building blocks and radiation dose rates in some dwellings in Ibadan, Nigeria, J. Environ. Radioact. 81 (1) (2005) 107–113.
[31] J.A. Ademola, Determination of natural radionuclides content in some building materials in Nigeria by gamma-ray spectrometry, Health Phys. 94 (1) (2008) 43–48.
[32] EC (European Commission), Radiological protection principles concerning the natural radioactivity of building materials, Radiat. Prot. 112 (1999) (Directorate General Environment. Nuclear Safety and Civil Protection).
[33] R.C. Smetsers, J.M. Tomas, A practical approach to limit the radiation dose from building materials applied in dwellings, in compliance with the Erratum Basic Safety Standards, J. Environ. Radioact. 196 (2019) 40–49.
[34] L. Rebegea, M. Dumitru, G. Rolea, D. Firescu, C. Serban, Dose rate in air for cylindrical shielded radioactive source, Int. Journal of Engineering Research and Application 7 (9) (September 2017) 2248–9622, pp.61–65.
[35] A.A. Abdulfattah, Effect of exposure buildup factors on reactor shielding, Al-Nahrain Journal of Science 13 (1) (2010) 78–83.
[36] F.M. Khan, J.P. Gibbons, Khan's the Physics of Radiation Therapy, Lippincott Williams & Wilkins, 2014.
[37] M. Orabi, Modelling the indoor radiation doses: a review and perspective, Radiat. Protect. Dosim. 185 (3) (2019) 282–295.
[38] M.Z. Anjum, S.M. Mirza, M. Tufail, N.M. Mirza, Z. Yasin, Natural radioactivity in building materials: dose determination in dwellings using hybrid Monte Carlo-deterministic approach, in: International Conference on Nuclear Data for Science and Technology, EDP Sciences, 2007, pp. 941–944.